An orbitally driven tropical source for abrupt climate change

Amy C. Clement, Mark A. Cane, and Richard Seager

Lamont-Doherty Earth Observatory, Palisades, New York

Abstract

Paleoclimatic data is increasingly showing that abrupt change is present in wide regions of the globe. Here we present a mechanism for abrupt climate change with global implications. Results from a tropical coupled ocean-atmosphere model show that under certain orbital configurations of the past, variability associated with El Niño/Southern Oscillation (ENSO) physics can abruptly lock to the seasonal cycle for several centuries producing a mean sea surface temperature (SST) change in the tropical Pacific which resembles a La Niña. We suggest that this change in SST would have a global impact and that abrupt events such as the Younger Dryas may be the outcome of orbitally driven changes in the tropical Pacific.

1. Introduction

Paleoclimatic records from high and low latitudes reveal that the climate has undergone abrupt changes in the past which can occur within decades (see Clark et al. 1999). There is no obvious external forcing of the climate that is so rapid. Abrupt changes, therefore, must arise from processes internal to the climate system or be the result of a rapid response to a gradual external forcing. Identifying the mechanisms that allow changes to be abrupt is essential for understanding the fundamental behavior of the climate and its sensitivity to forcing.

The Younger Dryas (YD), a rapid return to near glacial conditions lasting nearly a millenium during the last deglaciation, is an example of abrupt climate change. A common explanation for the YD is that meltwater pulses from the retreating Laurentide ice sheet flooded the North Atlantic with fresh water which led to an abrupt shut down (or weakening) of deep water formation, cooling the North Atlantic region, and explaining the return to near glacial conditions in various oceanic and terrestrial climate proxies there (see Alley and Clark 1999). High resolution records show that the onset and termination of this event occured within decades (Alley et al. 1993)

There are some fundamental problems with this view of the YD event: (1) There is a meltwater pulse both prior to the onset of the YD, and after the end of it (Fairbanks 1989). Further, some records indicate that deep water formation in the North Atlantic began to weaken several hundred years before the onset of the YD, and that the ocean circulation did not recover until after the termination of the event (Zhan et al. 1997, Moore et al. 1999). Also, modeling studies show that deep water formation can take several hundred years to respond to realistic meltwater inputs (Manabe and Stouffer 2000). (2) There is evidence for a YD age event from wide regions of the globe (e.g. Linsley and Thunell 1990, Denton and Hendy 1994, Lowell et al. 1995, Peteet 1995, Hughen et al. 1996, Thompson et al. 1995, 1998), yet models indicate that the impacts of changes in the Atlantic thermohaline circulation are confined mainly to the North Atlantic region with perhaps some effect in the Southern Ocean (Manabe and Stouffer 2000, Mikolajewicz et al. 1997).

On the other hand, changes in the tropical climate are known to have global impacts on interannual timescales, and are therefore a likely candidate for generating global climate change on longer timescales. Here we investigate the behavior of the tropical climate system using an idealized model, and suggest that coupled ocean-atmosphere interactions are a potential source for abrupt global change.

2. Modeling Experiments

The model we use was developed by Zebiak and Cane (1987). It involves only coupled ocean-atmosphere interactions in the tropical Pacific, includes linear dynamics in the ocean and atmosphere, but with non-linear atmosphere and ocean thermodynamics. For the standard set of parameters, the behavior of ENSO in the model is similar to the real world and can be described as a quasi-periodic, irregular oscillation that is partially phase-locked to the seasonal cycle.

Here, we investigate how changes in the seasonal cycle related to the Earth's orbital parameters (Berger 1978) impact ENSO. The model is forced with orbitally induced changes in the seasonal cycle of solar forcing over the last 500 kyr (Figure 2a) which are imposed as an anomalous heat flux into the ocean. Under particular orbital configurations, ENSO variability "flickers" on and off, abruptly locking to the seasonal cycle for several centuries. Figure 1a shows an example of one such period that occurs at approximately 12 kyr, a time which coincides with the YD. There is a mean SST change associated with this shut down in ENSO (Figure 1b) which has an increased zonal gradient, similar to that of a La Niña event. The abrupt events are paced by the solar forcing and recur approximately every 11 kyr (Figure 2a,b). During the periods 450-400 and 50-0 kyr, the ENSO shut downs last for several centuries. At these times the orbital configuration is similar because of the 400 kyr cycle in eccentricity.

To aid in understanding the link between the orbital forcing and the abrupt behavior of ENSO, we decompose the solar forcing into empirical orthogonal functions (EOFS). The first two EOFs (Figure 3a,b) explain 50 and 48 % of the total variance, and the principal components (PCs) are shown in Figure 3c with times of ENSO shut downs longer than 20 years indicated by bars. These two EOFS describe the precession through the year of the perihelion, the point in the orbit where the Earth is closest to the Sun, which varies on a 22 kyr timescale. When PC1 is positive maximum perihelion occurs in boreal summer; when PC2 is positive maximum perihelion occurs in boreal spring. We note that positive values for PC2 constitute an effective strengthening of the seasonal cycle in the equatorial Pacific, where maximum SSTs occur in April and minimum in October.

We examine the behavior of ENSO as a function of of these two parameters (PC1 and PC2) which fully describe the solar forcing. Viewed this way, the character of ENSO shows two fairly distinct regimes of behavior (Figure 4). When the seasonal cycle strength is increased relative to the modern (PC2 $>$ 0), the oscillation is strong, highly regular, and has a dominant period of 3 years. Similar results have been shown in previous studies (Chang et al. 1994, Jin et al. 1996). When the seasonal cycle is damped (PC2 $<$ 0), the oscillation is strong, with a main dominant period of the familiar 4 years, but is fairly irregular with power spread over a wider range of periods. (When the seasonal cycle is greatly damped (PC2 $<$ -0.1), there is a shift to the three year period, but the system spends little time in this orbital configuration.)

The ENSO shut downs (shown as black circles in Figure 4) occur during the transition between the two regimes of (1) a highly regular oscillation at a 3 year period (PC2 $>$ 0) and (2) a more irregular oscillation with a dominant period of 4 years (PC2 $<$ 0). For this orbital configuration, there is a minimum in total variance and the oscillation is moderately regular. At this point, the system has no clearly defined mode of behavior and episodically locks to the period of the forcing (1 year). This transition period occurs when perihelion is in either winter or summer seasons, thus giving a return period for the ENSO shut downs of 11 kyr, or half a precessional cycle.

The maximum length of the shut downs of ENSO occur when eccentricity is weak (Figure 2a,b). That is, the system spends more time in this "transition" zone when the potential for locking to the seasonal cycle is high. It is also notable that the shut downs do not occur for each of these optimal orbital configurations (Figure 2a,b). We compile the results for 14 runs over the period 13-11 kyr to evaluate the statistics of shut downs at this time. In a control run of 60,000 years with orbital parameters set at modern values, the maximum length of ENSO shut downs in 2000 year periods never exceeds 30 year. In the multiple runs for the 13-11 kyr forcing, 9 out of the 14 2000-year runs have shut downs lasting longer than 30 years, and the lengths of these are nominally 30, 33, 43, 56, 123, 125, 140, 213 and 309 years. The forcing therefore has the effect of making the system more likely to undergo these shut downs in ENSO every 11 kyr when the system is moderately irregular and has a minimum total variance. However, a long shut down is not guaranteed to happen, and has no preferred timescale.

In order to test the robustness of this mechanism for abrupt change, we perform further experiments in which the drag coefficient (C_d) of the model is altered. This parameter is used in the standard bulk formula to calculate the surface wind stress anomalies, and controls the effective dynamical coupling between the ocean and atmosphere. Tziperman et al. (1994) have studied the behavior of the ENSO system (under the modern orbital configration) in response to changes in this parameter. For C_d = 90-100%, the model is in a chaotic regime; with C_d = 80%, the system is mode locked; for lower values, there is no coupled instability, and therefore no oscillation. We explore the additional case for C_d = 110%, the modern ENSO behavior is much stronger (the power is almost doubled), and slightly less irregular as in the standard case.

Under the orbital forcing, when C_d is reduced to 90%, the regimes of ENSO behavior shown in Figure 4 are qualitatively similar, however the power in the interannual band is about half that for the standard value because of the weaker coupling between the ocean and atmosphere. During the transition period between the two regimes the orbital forcing has more effect, and the shut downs are more dramatic, lasting for entire milennia at times (Figure 2c). For C_d values smaller than 90%, the interannual variability is entirely damped out and the system follows the forcing smoothly over time. When C_d is increased to 110% of the control value, Figure 4 is again qualitatively similar to that of the standard value of C_d. However, since the effective coupling is increased, the oscillation is considerably stronger, and the solar forcing has less effect on the system. The system goes through periods of minimum variance for the same orbital configurations as the control run but does not lock to a seasonal cycle.

The values of C_d for which the ENSO shut downs occur (90-110%) place the model in a non-linear dynamical regime. There is currently considerable debate about the degree to which the real world ENSO system can be described as a non-linear process versus a linear stochastic process (Neelin et al. 1998). We perform additional experiments in which C_d is reduced to 80% of the control value and add temperature perturbations that are random in space and time with a standard deviation of 0.2 ^{o} C (as in Thompson and Battisti 2001). In this configuration, the model behaves more like a linear, stochastically driven system, though it is not perfectly linear. In this case, locking to the seasonal cycle in this case does not occur because of the noise in the system. However, the ENSO system goes through generally similar periods of abruptly reduced variance as in the run with the standard value of C_d, though the drop in variance is less dramatic in the case with noise (Figure 5).

3. Discussion and Conclusions

The results presented here provide a quantitative demonstration of how orbital forcing, which varies smoothly over time, can provoke an abrupt climate response. Two regimes of ENSO behavior are identified for different orbital configurations in which the total power, period and regularity of the oscillation are distinct. When the ENSO oscillation is in transition between the two regimes, and is weak and moderately regular, the system can lock to the period of the forcing (1 year). This gives rise to the abrupt behavior shown in Figure 1. This behavior recurs on an approximately 11 kyr timescale, when perihelion occurs either during boreal winter or summer.

The character of the abrupt change depends on the value of C_d, as well as the presence of noise. The abruptness of the response to the solar forcing is more dramatic in the non-linear cases, though is still notable in the case with noise. At this stage, it is difficult to discern from the short observational how non-linear the real world ENSO is. Nevertheless, in all cases shown here, the system goes through abrupt reductions in variance which occur on a shorter timescale than that of the forcing. This suggests that the tropical Pacific coupled ocean-atmosphere system contains the physics that are capable of generating an abrupt response to a smoothly varying forcing.

The paleoclimate record shows that the pacing of abrupt climate change could be linked to the solar forcing. Heinrich (1988) found that episodes of major ice rafting in the North Atlantic recur on an 11 kyr timescale over the last glacial at times of boreal winter and summer insolation maxima, as in the results shown here. Bond et al. (1999) show that the timing between the ice rafting events decreases as the Earth moves into full glacial conditions, but that earlier in the glacial, these detrital events occur on a roughly 11 kyr timescale (G. Bond, personal communication). Our results raise the possibility that the YD is the return to these orbitally paced events once the influence of the ice sheets is diminished.

Using an AGCM, Yin and Battisti (2000) show that an increase in the equatorial Pacific SST gradient, such as occurs in our model at the time of the YD, can have a large influence over North America, and cause melting at the Southern margin of the Laurentide ice sheet. Schmittner et al. (2000) used modern observations and models to show that during La Niña events reduced freshwater export from the tropical Atlantic could slow the Atlantic thermohaline circulation. These studies suggest ways in which the climate in the North Atlantic region can change in response to a La Niña-like SST change at the time of the YD. The YD climate event appears differently around the globe (e.g. Peteet 1995). We suggest that a persistent La Niña-like SST change would have some pattern associated with it that could be compared with the paleoclimate indicators for that time.

The model used in this study is highly idealized (see Clement et al. 1999 for further discussion). More complete models are needed to test the influence of additional processes on the mechanism proposed here. We note that the modern ENSO (zero forcing) is close to the transition period during which abrupt ENSO shut downs can occur, suggesting that currently ENSO may be fairly sensitive to external forcing. Further investigation into the link between abrupt climate changes and orbital forcing of the past, both from a modelling and observational perspective, is clearly important for understanding the nature of abrupt climate change, and also for evaluating the possible future behavior of ENSO.

4. Acknowledgments

The authors thank S. Zebiak and G. Bond for insightful comments and discussions. The comments of the two reviewers is also gratefully appreciated. This work was funded by NSF Grant ATM99-86515 and NOAA grant UCSIO PO 10156283 (The Consortium on the Oceans Role in Climate).

References

Alley, R. and Clark, P., 1999: The deglaciation of the Northern Hemisphere: a global perspective. *Ann. Rav. Earth Planet. Sci.*, **27**, 149–182.

Alley, R., Meese, D. A., Shuman, C., Gow, A., Taylor, K., Grootes, P., White, J., Ram, M., Waddington, E. D., Mayewski, P., and Zielinski, G., 1993: Abrupt increase in Greenland snow accumulation at the end of the Younger Dryas event. *Nature*, **362**, 527–529.

Berger, A., 1978: Long-term variations of daily insolation and Quaternary climate changes. *J. Atmos. Sci.*, **35**, 2362–2367.

Bond, G., Showers, W., Elliot, M., Evans, M., Lotti, R., Hajdas, I., Bonani, G., and Johnson, S., 1999: The North Atlantic's 1-2 kyr climate rhythm: Relation to Heinrich events, Dansgaard/Oeschger cycles and the Little Ice Age. In P. U. Clark and R. S. Webb and L.D. Keigwin, editor, *Mechanisms of millenial scale global climate change*, pp. 35–57. American Geophysical Union, Washington.

Chang, P., Wang, B., Li, T., and Ji, L., 1994: Interactions between the seasonal cycle and the Southern Oscillation: Frequency entrainment and chaos in a coupled ocean-atmosphere model. *Geophys. Res. Lett.*, **21**, 2817–2820.

Clark, P.U. and R. S. Webb and L.D. Keigwin, 1999: *Mechanisms of millenial scale global climate change*. American Geophysical Union, Washington.

Clement, A. C., Seager, R., and Cane, M. A., 1999: Orbital controls on the tropical climate. *Paleoceanography*, **14**, 441–456.

Denton, G. and Hendy, C., 1994: Younger Dryas age advance of Franz Josef Glacier in the Southern Alps of New Zealand. *Science*, **264**, 1434–1437.

Fairbanks, R. G., 1989: A 17,000 year glacio-eustatic sea-level record: Influence of glacial melting rates on the Younger Dryas and deep ocean circulation. *Nature*, **342**, 637–642.

Heinrich, H., 1988: Origin and consequences of cyclic ice rafting in the Northeast Atlantic ocean during the past 130,000 years. *Quat. Res.*, **29**, 142–152.

Hughen, K., Overpeck, J., Peterson, L., and Trumbore, S., 1996: Rapid climate changes in the tropical Atlantic region during the last deglaciation. *Nature*, **380**, 51–54.

Jin, F.-F., Neelin, J. D., and Ghil, M., 1996: El Niño/Southern Oscillation and the annual cycle: subharmonic frequency-locking and aperiodicity. *Physica D*, **98**, 442–465.

Linsley, B. and Thunell, R., 1990: The record of deglaciation in the Sulu Sea: Evidence for the Younger Dryas event in the tropical western Pacific. *Paleoceanography*, **5**, 1025–1039.

Lowell, T., Heusser, C., Anderson, B., Moreno, P., Hauser, A., Heusser, L., Schluchter, C., Marchant, D., and Denton, G., 1995: Interhemispheric correlation of late Pleistocene glacial events. *Science*, **269**, 1541–1549.

Manabe, S. and Stouffer, R., 2000: Study of abrupt climate change by a coupled ocean-atmosphere model. *Quat. Sci. Rev.*, **19**, 285–299.

Mikolajewicz, U and T.J. Crowley and A. Schiller and R. Voss, 1997: Modelling teleconnections between the North Atlantic and the North Pacific during the Younger Dryas. *Nature*, **387**, 384–387.

Moore, T., Walker, J., Rea, D., Lewis, C., Shane, L., and Smith, A. J., 2000: Younger Dryas interval and outflow from the Laurentide ice sheet. *Paleoceanography*, **15**, 4–18.

Neelin, J. D., Battisti, D., Hirst, A., Jin, F., Wakata, Y., Ymamgata, T., and Zebiak, S., 1998: ENSO theory. *J. Geophys. Res.*, **103**, 14,261–14,290.

Peteet, D., 1995: A global Younger Dryas. *Quat. Intl.*, **28**, 93–104.

Schmittner, A., Appenzeller, C., and Stocker, T. F., 2000: Enhanced Atlantic freshwater export during El Niño. *Geophys. Res. Letts.* in press.

Thompson, C. J. and Battisti, D., 2001: A Linear Sochastic Dynamical Model of ENSO. Part II: Analysis. *J. Climate*, p. in press.

Thompson, L., Davis, M. E., Mosley-Thompson, E., Sowers, T. A., Henderson, K. A., Zagorodnov, V. S., Lin, P.-N., Mikhalenko, V. N., Campen, R. K., Bolzan, J. F., Cole-Dai, J., and Francou, B., 1998: A 25,000-Year Tropical Climate History from Bolivian Ice Cores. *Science*, **282**, 1858–1864.

Thompson, L., Mosley-Thompson, E., Davis, M. E., Lin, P.-N., Henderson, K. A., Cole-Dai, J., Bolzan, J. F., and b. Liu, K., 1995: Late Glacial Stage and Holocene Tropical Ice Core Records from Huascaran, Peru. *Science*, **269**, 46–50.

Tziperman, E., Cane, M. A., and Zebiak, S. E., 1994: Irregularity and locking to the seasonal cycle in an ENSO prediction model as explained by the quasi-periodicity route to chaos. *J. Atmos. Sci.*, **52**, 293–306.

Yin, J. and Battisti, D., 2000: The importance of tropical sea surface temperature patterns in simulations of the Last Glacial Maximum climate. *J. Climate*, p. in press.

Zahn, R., Kudrass, H., Park, M., Erlenkeuser, H., and Gootes, P., 1997: Thermohaline instability in the North Atlantic during meltwater events: stable isotope and ice-rafted detritus records from core SO75-26KL, Portugese margin. *Paleoceanography*, **12**, 696–710.

Zebiak, S. E. and Cane, M. A., 1987: A model El Niño-Southern Oscillation. *Mon. Weather. Rev.*, **115**, 2262–2278.

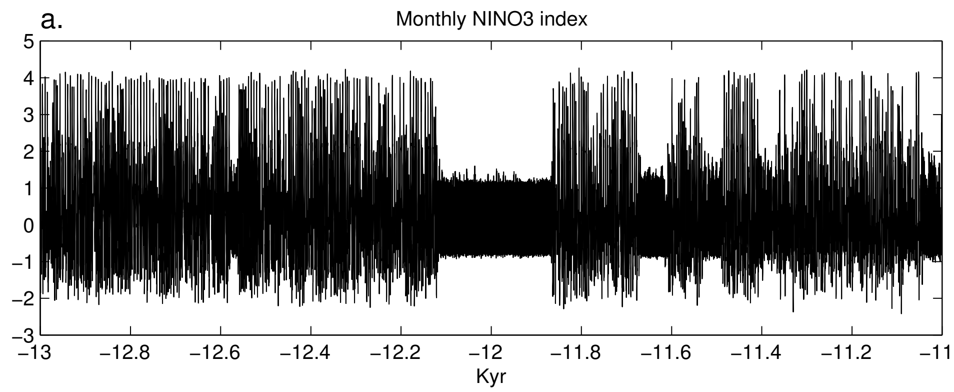
a.
Monthly NINO3 index
5
4
3
2
1
0
−1
−2
−3
−13
−12.8
−12.6
−12.4
−12.2
−12
−11.8
−11.6
−11.4
−11.2
−11
Kyr

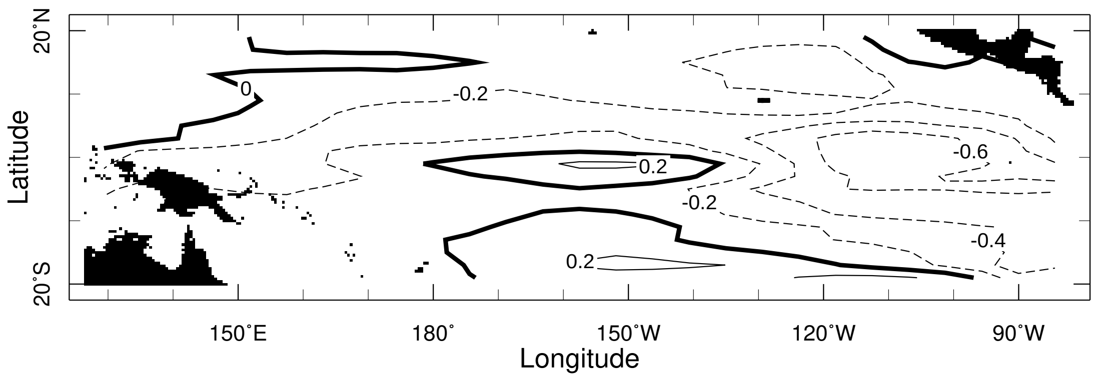
20°N
20°S
Latitude
0
-0.2
0.2
-0.6
-0.4
150°E
180°
150°W
120°W
90°W
Longitude

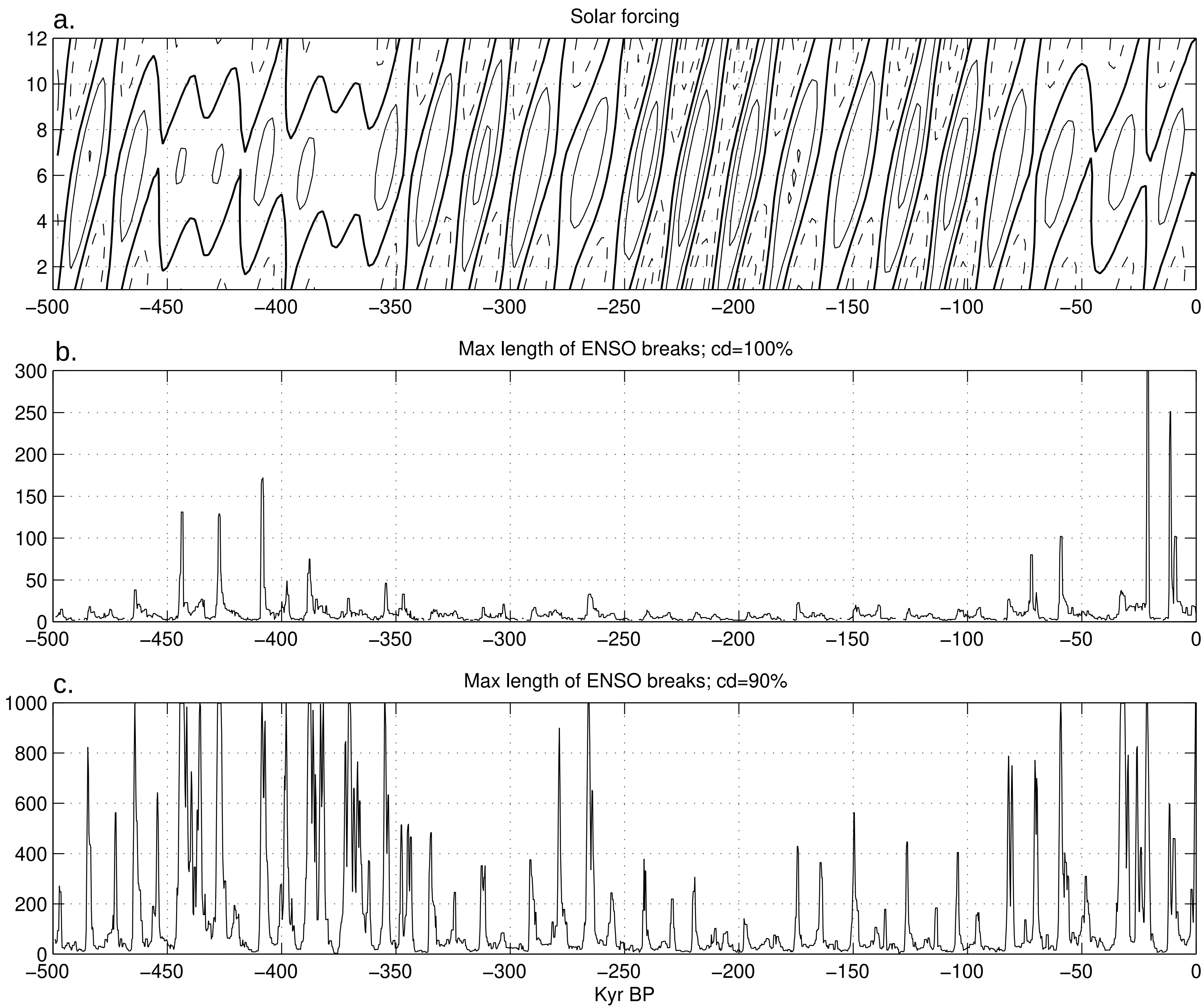
a.
Solar forcing
12
10
8
6
4
2
−500
−450
−400
−350
−300
−250
−200
−150
−100
−50
0
b.
Max length of ENSO breaks; cd=100%
300
250
200
150
100
50
0
c.
Max length of ENSO breaks; cd=90%
1000
800
600
400
200
0
Kyr BP

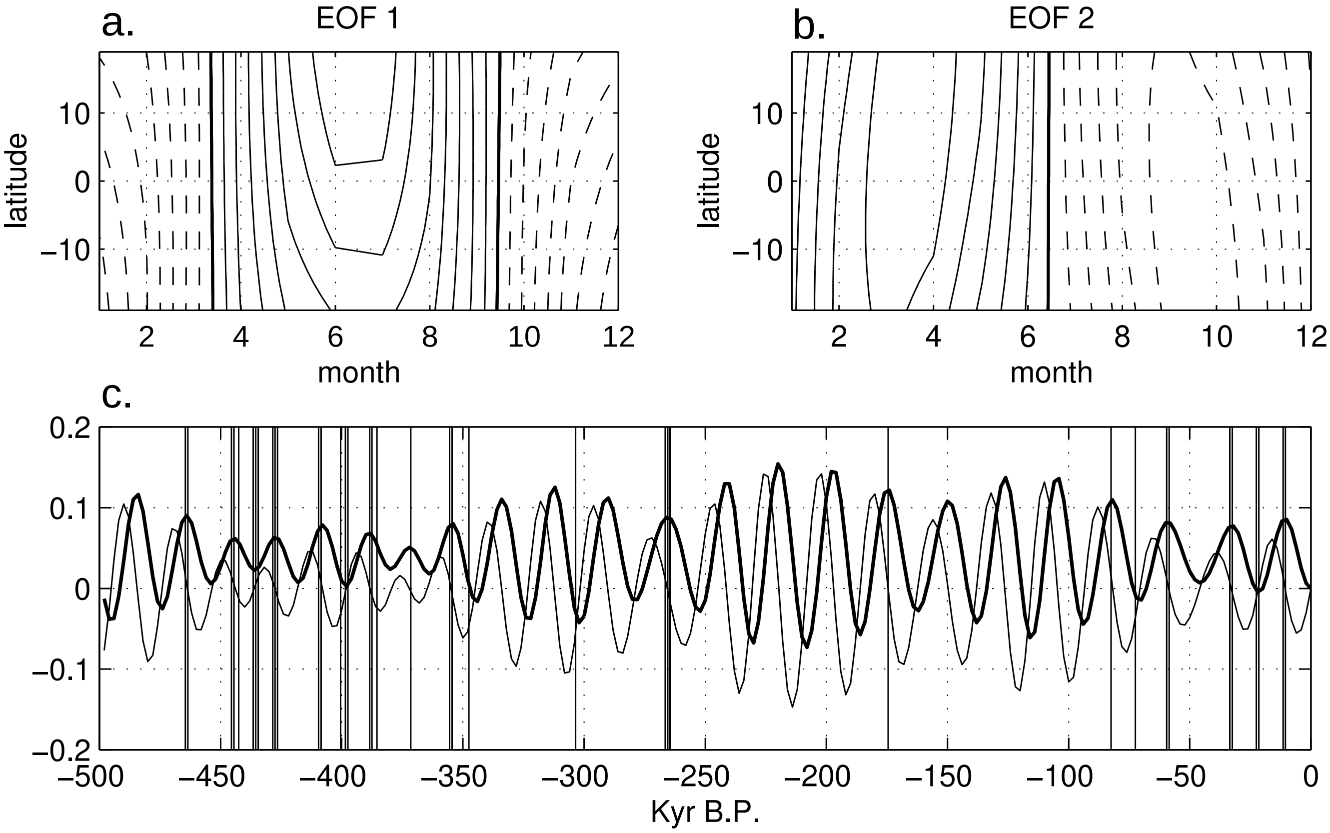
a.
EOF 1
latitude
month
b.
EOF 2
latitude
month
c.
Kyr B.P.

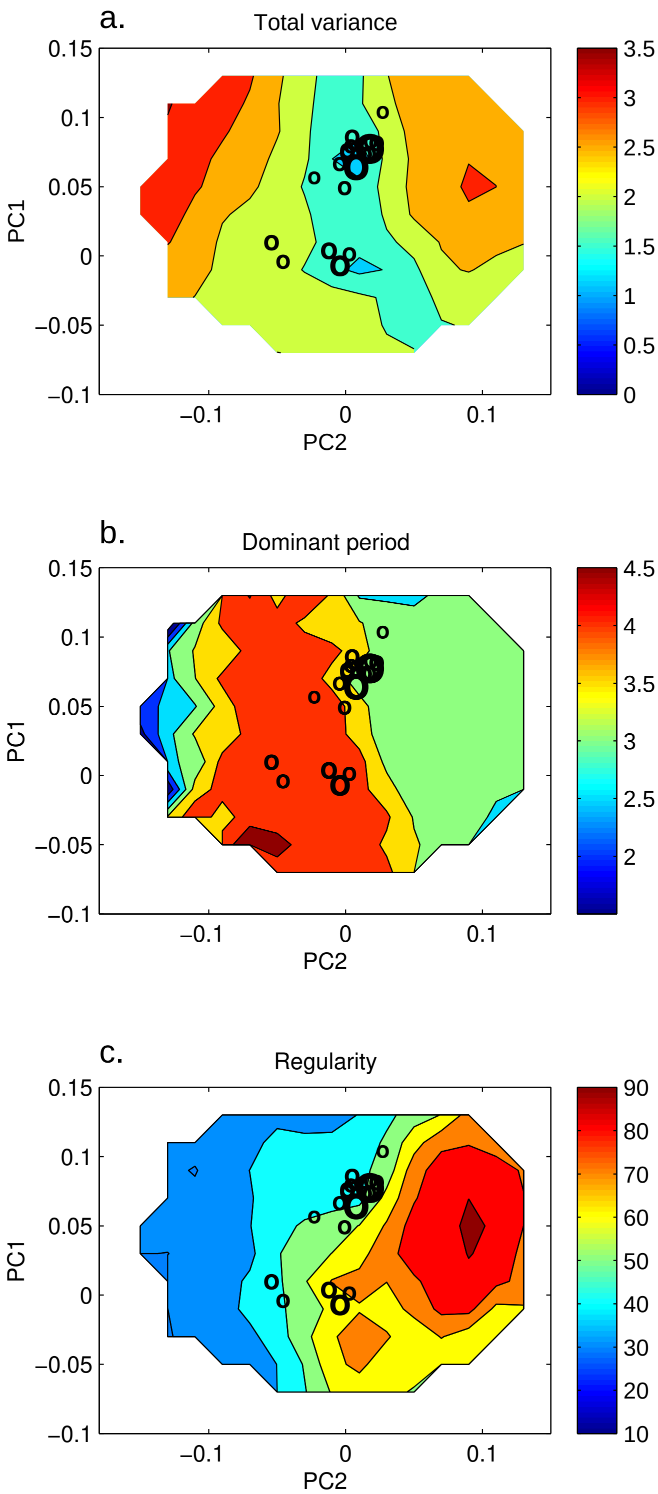
a.
Total variance
PC1
PC2
b.
Dominant period
PC1
PC2
c.
Regularity
PC1
PC2

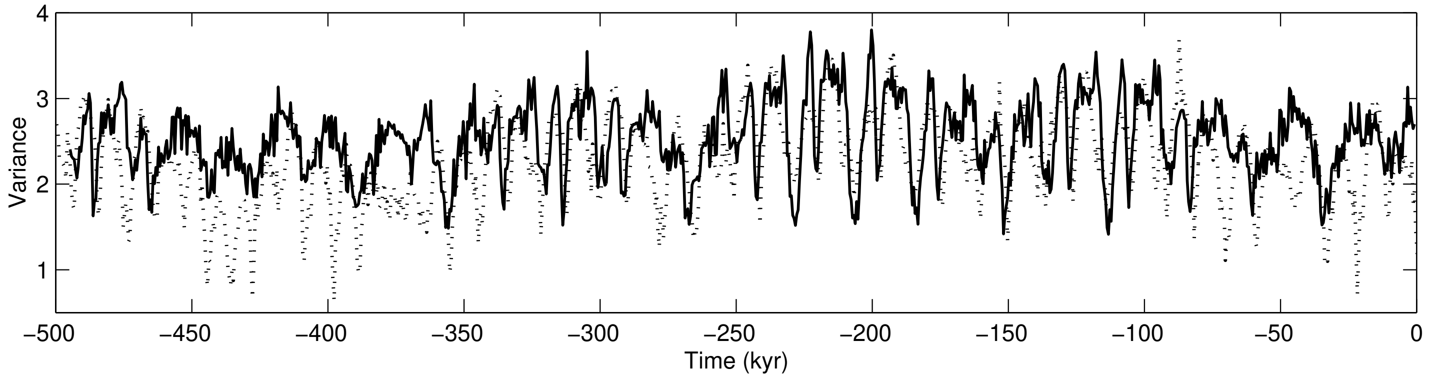

5

Figure Captions

Figure 1. (a) Monthly NINO3 index (^oC) from the Zebiak-Cane coupled model with imposed orbital forcing for the period between 13 and 11 kyr before present. (b) Annual mean SST change (^oC) relative to the control run for 12 kyr when ENSO is shut down.

Figure 2. (a) Solar forcing on the equator imposed as an anomalous heat flux into the ocean in the Zebiak-Cane coupled model for the last 500 kyr as a function of kyr BP (x-axis) and month of the year (y-axis). The contour interval is 20 Wm^{-2}. Solid lines indicate heat flux into the ocean and dashed lines indicate heat flux out of the ocean. (b) Maximum length of shut downs of ENSO (years) in 1000 year overlapping windows for the standard value of the C_d. A shut down is defined to occur when the annual mean NINO3 does not exceed 0.5 ^oC for longer than 5 years. (c) Same as (b) except for the run with C_d reduced to 90 % of its standard value.

Figure 3. (a) First EOF (50 % of variance) of the solar forcing as a function of month (x-axis) and latitude (y-axis). (b) Second EOF (48 % of the variance). (c) Principal Component of EOF1 (bold solid line) and EOF2 (light solid line). Overlain on this (black vertical bars) are the times of shut down of ENSO (for the standard value of C_d- see Figure 2b) that last longer than 25 years.

Figure 4. (a) Contour plot of the total variance ($^oC^2$) of the monthly NINO3 index as a function of PC2 (x-axis) and PC1 (y-axis), (b) dominant period (years), and (c) percent of interannual variance (annual variance removed) in the dominant period, or "regularity" of the oscillation. For this latter statistic, we pick the dominant frequency and then sum the power at that period and the two adjacent periods. The values of PC1 and PC2 for which ENSO shut downs are longer for than 25 years are indicated by black circles. The size of the circle is proportional to the length of the shut down.

Figure 5. Variance ($^oC^2$) of the NINO3 index in 1000 year windows for the case of C_d at the standard value (dotted), and for the case with C_d = 80% with white noise forcing (heavy solid).